Вісник Тернопільського національного технічного університету
https://doi.org/10.33108/visnyk_tntu
Scientific Journal of the Ternopil National Technical University
2024, № 2 (114) https://doi.org/10.33108/visnyk_tntu2024.02
ISSN 2522-4433. Web: ***visnyk.tntu.edu.ua***

УДК 539.4 : 629.5

STUDY OF INFLUENCE OF THE AUXILIARY FACTORS ONTO CHARACTERISTICS OF ELASTIC-PLASTIC DEFORMATION IN THE STRESS CONCENTRATOR OF THE BEAM-WALL WITH BROKEN EDGES

Valerii Sokov

Admiral Makarov National University Of Shipbuilding, Mykolaiv, Ukraine

Summary. *The thin-walled steel beam-wall with broken edges is being investigated, which is a part of many structures. The wall of this beam consists of two prismatic parts with a linear transition from a smaller to a larger wall height, together forming an angular upper edge with the edges of the prismatic parts. The lower linear edge of the wall is attached to the sheathing.The beam-wall is subjected to static and cyclic loads, under which elastic-plastic strains may occur in the stress concentrator. This leads to failure of static strength and growth of fatigue cracks. The factors influencing the parameters of elastic-plastic deformation in the stress concentrator of this beam are practically unstudied. The article under discussion presents the results of studying the influence of the beam-wall thickness and load vector balancing on the values of static and cyclic ranges of elastic-plastic strains in the stress concentrator. It had been found that load vector balancing significantly improves the results of elastic-plastic strains under single static loading and allows for the use of a larger load increment to achieve the same results as when no balancing is applied. Applying load vector balancing stabilizes the cyclic deformation loop practically from the first cycle. If balancing is absent, stabilization occurs only from the third cycle. Unlike static ones, the values of cyclic ranges do not depend on the application or non-application of balancing and remain practically stable with fixed geometric parameters and loading. Gradual reduction in the thickness of the beam-wall causes an increase in the range (static and cyclic) of elastic-plastic strains in the stress concentrator. The obtained results will shorten the time required for planning serial calculations of elastic-plastic deformation of the beam-wall with broken edges to develop appropriate design techniques.*

Key words: *elastic-plastic deformation, cyclic diagrams, beam with broken edges, finite elements.*

https://doi.org/10.33108/visnyk_tntu2024.02.060 *Received 27.03.2024*

1. Introduction. The beam-wall with broken edges in Fig. 1 is a component of ship hulls, civil, and industrial structures. This beam has a lower straight edge *2* attached to the sheathing *I*, while the upper broken edge is free.

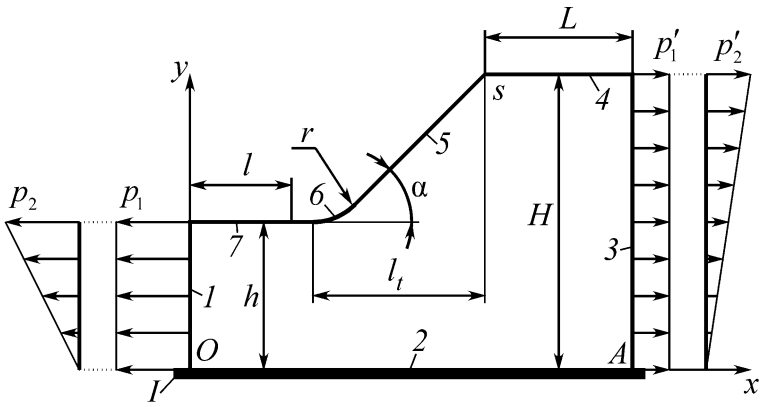

Figure 1. The general view of the beam-wall

 Corresponding author: Valerii Sokov; e-mail: valeriy.sokov@nuos.edu.ua

The beam-wall in Fig. 1 is subjected to axial p1 and bending p2 loads. Axial loads p1 may arise, for example, from the overall bending of the ship's hull, while bending loads p2 from local bending of the deck.

Beams of this type can operate under both static and cyclic loading conditions, both in elastic and elastic-plastic deformation modes. The investigated beam operates under conditions where elastic-plastic deformation in the stress concentrator cannot always be avoided. For example, if such a beam-wall is part of floating structures or a ship's hull, elastic-plastic deformation in the concentrator is provided by the following ship operations: loading-unloading, placing the vessel in the dock, extreme wave loading, etc. The occurrence of plastic strains in the stress concentrator 6 (Fig. 1) leads to static strength failure, while cyclic loading induces the appearance and growth of fatigue cracks in the concentrator.

Currently, there are no systematic methods for assessing the strength and durability of such beam-walls (Fig. 1), and accordingly, no design recommendations for them. The primary need is to study the factors influencing the parameters of elastic-plastic deformation in the concentrator 6 of the beam-wall in Fig. 1. Investigating these factors will help shorten the planning and execution time of serial calculations for the beam-wall under conditions of elastic-plastic deformation.

2. Analysis of the literature and problem statement. First of all, a review of the literature is dedicated to examining implementations of plastic flow theory models. The work [1] presents a considerable number of different implementations of plastic flow theory up to 2005, where their advantages and disadvantages had been discussed. Some schemes from the work [1] were implemented and discussed within the scope of this research.

Currently, plastic flow dependencies are mainly based on associative, non-associative, and fractional-order laws. Associative and non-associative laws are well-known from classical literature (see, for example, [1]) and are not discussed here. One of the new directions, which is quickly developing, is the fractional-order plastic flow law or fractional plastic flow rule [2, 3], which is generally obtained by defining fractional derivatives from the plasticity surface. The works [2, 3] propose general schemes and models of plastic flow based on fractional-order plastic flow laws, which depend on parameters and demonstrate a high correlation between numerical and experimental results. Implementation and comparison of fractional-order plastic flow laws among themselves and with classical associative laws require time. However, as shown in [1], associative plastic flow laws are quite accurate for metals, and their implementation is relatively simple, which encourages the implementation of associative laws in the mathematical model of plastic flow for research purposes.

In article [4], an improved CE/SE (the space-time Conservation Element and Solution Element method) scheme is proposed, extended to solve problems of elastic-plastic flow based on hexahedral mesh. CE/SE methods are new high-precision CFD methods for hyperbolic conservative systems. It is unclear how CE/SE methods can account for unloading, strengthening effects, Bauschinger effect, etc. CE/SE methods are not adapted for calculations of non-conservative systems, which occur under complex loading conditions, unlike the plastic flow theory.

In article [5], the problem of volumetric locking is described, which occurs for low-order finite elements (FE) when the plastic volume gradually increases in the structure under increasing external loads. To overcome the problem of volumetric locking in [5], it is recommended to either use high-order FE or apply special adaptive algorithms for low-order FE, including the p-adaptive scheme. The presence of volumetric locking will be examined in the research part of this article.

The investigated beam-wall in Fig. 1 is a thin-walled structure, in which, under elastic deformation and given loading conditions, a two-dimensional stress state is realized. However, the plate thickness affects the characteristics of elastic-plastic deformation under other equal conditions, as numerically and experimentally demonstrated in works [6, 7, 8]. This prompts

the study of the influence of thickness s on the magnitudes of elastic-plastic strains in the stress concentrator 6 (Fig. 1) and not to consider the problem as entirely two-dimensional.

In determining the characteristics of plastic deformation, the type of two-dimensional stress state matters: plane strain or plane stress [8, 9, 10, 11, 12]. If the plane strain model is adopted, then the radius of the plastic zone is three times smaller than if the plane stress model is adopted [8, p. 81]. In [9, 10, 11, 12], plastic deformation under conditions of plane strain and plane stress are distinguished, and proper conclusions are drawn accordingly. In particular, in publication [10], it is noted that the results were verified using a volumetric problem. The works [8–12] additionally suggest applying a volumetric solid mechanics problem to the investigated beam-wall in Fig. 1.

Literature review has shown that unresolved issues for the beam-wall in Fig. 1 include determining the influence of thickness, the type of two-dimensional stress-strain state (plane strain or plane stress), the type of FE, and peculiarities of the plastic flow model on the parameters of elastic-plastic deformation. To solve these problems, it is necessary to adopt a volumetric model and an associative plastic flow law.

3. Purpose and objectives of the investigation. The aim of the study is to investigate the numerical and physical parameters affecting the magnitude of static and cyclic elastic-plastic strains in the stress concentrator of the beam-wall, which will enable tuning parameters for serial calculations.

To achieve the stated aim, the following problems need to be solved:

– present a model of plastic flow theory, describe the calculation technique, and determine the influence of the FE type on the results;

– for fixed geometric parameters of the beam-wall, calculate the static and cyclic ranges of elastic-plastic strains in the presence and absence of load vector balancing and draw appropriate conclusions;

– establish the dependency of cyclic elastic-plastic strains' ranges in the stress concentrator of the beam-wall on its thickness for fixed geometric parameters.

4. Materials and methods of the investigation. The research method employed is the Finite Element Method (FEM), implemented by the author in the C++ programming language, which allows solving problems of both volumetric elasticity theory and plastic flow. FE of tetrahedral shape with 10 nodes [13] and 20 nodes [14] were utilized, corresponding to quadratic and cubic displacement approximations, respectively. The stress concentrator *6* of the beam-wall with broken edges (Fig. 1) serves as the object of investigation. The parameters of elastic-plastic deformation in this concentrator constitute the subject of the study.

5. Results of the research on the influence of factors on parameters of elastic-plastic deformation.

5.1. Plastic flow theory model. Within the scope of this research, the mathematical model of plastic flow theory was implemented within the framework of the elastic solutions method, as described in [15], which is a variant of the initial stress method [16]. Increments of (generalized) nodal displacements $\Delta\mathbf{q}$ are determined through an iterative process [1], which is carried out on the FE model.

$$\left.\begin{aligned}
&\mathbf{K}\cdot\Delta\mathbf{q}_{n,i}=\Delta\mathbf{Q}_n+\mathbf{Q}_{n-1}^{\text{unb}},\quad \Delta\mathbf{Q}_n=\Delta\mathbf{R}_n+\mathbf{K}_{\text{pf},n}\cdot\Delta\mathbf{q}_{n,i-1},\\
&\mathbf{K}_{\text{pf},n}=\int_V\mathbf{B}^T\cdot\mathbf{D}_{\text{pf},n}\cdot\mathbf{B}dV,\quad \mathbf{Q}_{n-1}^{\text{unb}}=\mathbf{Q}_{n-1}^{\text{ext}}-\int_V\mathbf{B}^T\cdot\boldsymbol{\sigma}_{n-1}dV,\\
&\mathbf{Q}_{n-1}^{\text{ext}}=\sum_{j=1}^{j=n-1}\Delta\mathbf{R}_j.\\
&i=1,2,\ldots;\quad n=1,2,\ldots,N_P;\quad \Delta\mathbf{q}_{n,i=0}=0,
\end{aligned}\right\}\qquad(1)$$

where

$$
\left.
\begin{aligned}
&\mathbf{K} = \int_V \mathbf{B}^{\mathrm{T}} \cdot \mathbf{D} \cdot \mathbf{B} dV, \\
&\boldsymbol{\varepsilon} = \{\varepsilon_x, \varepsilon_y, \varepsilon_z, \gamma_{xy}, \gamma_{yz}, \gamma_{zx}\} = \mathbf{B} \cdot \Delta\mathbf{q}, \quad \boldsymbol{\sigma} = \{\sigma_x, \sigma_y, \sigma_z, \tau_{xy}, \tau_{yz}, \tau_{zx}\} = \mathbf{D} \cdot \boldsymbol{\varepsilon}, \\
&f(\boldsymbol{\sigma}) = f(\sigma_x, \sigma_y, \sigma_z, \tau_{xy}, \tau_{yz}, \tau_{zx}) = \\
&= (\sigma_x - \sigma_y)^2 + (\sigma_y - \sigma_z)^2 + (\sigma_z - \sigma_x)^2 + 6(\tau_{xy}^2 + \tau_{yz}^2 + \tau_{zx}^2) - 2\sigma_s^2, \\
&\mathbf{a} = \left(\frac{\partial f}{\partial \boldsymbol{\sigma}}\right) = \left\{\frac{\partial f}{\partial \sigma_x}, \frac{\partial f}{\partial \sigma_y}, \frac{\partial f}{\partial \sigma_z}, \frac{\partial f}{\partial \tau_{xy}}, \frac{\partial f}{\partial \tau_{yz}}, \frac{\partial f}{\partial \tau_{zx}}\right\} = \\
&= \left\{2(2\sigma_x - \sigma_y - \sigma_z), 2(2\sigma_y - \sigma_z - \sigma_x), 2(2\sigma_z - \sigma_x - \sigma_y), 12\tau_{xy}, 12\tau_{yz}, 12\tau_{zx}\right\}, \\
&\mathbf{D}_{\mathrm{pf},n} = \begin{cases} \dfrac{\mathbf{D} \cdot \mathbf{a} \cdot \mathbf{a}^{\mathrm{T}} \cdot \mathbf{D}}{A + \mathbf{a}^{\mathrm{T}} \cdot \mathbf{D} \cdot \mathbf{a}}, & \text{if} \quad f(\boldsymbol{\sigma}_{n-1}) \geq 0, \\ 0, & \text{if} \quad f(\boldsymbol{\sigma}_{n-1}) < 0, \end{cases}
\end{aligned}
\right\} \qquad (2)
$$

in this case

$$
\mathbf{D} = G \begin{bmatrix}
\frac{2(1-\mu)}{1-2\mu} & \frac{2\mu}{1-2\mu} & \frac{2\mu}{1-2\mu} & 0 & 0 & 0 \\
\frac{2\mu}{1-2\mu} & \frac{2(1-\mu)}{1-2\mu} & \frac{2\mu}{1-2\mu} & 0 & 0 & 0 \\
\frac{2\mu}{1-2\mu} & \frac{2\mu}{1-2\mu} & \frac{2(1-\mu)}{1-2\mu} & 0 & 0 & 0 \\
0 & 0 & 0 & 1 & 0 & 0 \\
0 & 0 & 0 & 0 & 1 & 0 \\
0 & 0 & 0 & 0 & 0 & 1
\end{bmatrix}, \qquad (3)
$$

Explanation to formulae (1), (2), (3) are given in the Table 1.

Table 1

Explanations to formulae (1), (2), (3)

№	Explanation
1	2
1	i – iteration number
2	n – step number of loading
3	N_P – number of loading steps
4	**K** – elastic stiffness matrix, which remains constant throughout the entire iterative process
5	V – domain of integration restricted by the volume of the structural element (FE).
6	**B** – geometric matrix that relates strains to nodal displacements or their increments
7	**D** – elastic matrix specified by the formula (3)
8	G – shear modulus

The end of the table

№	Explanation
1	2
9	μ – Poisson's ratio
10	$\Delta\mathbf{q}_i$, $\Delta\mathbf{q}_{i-1}$ – increments of nodal displacements
11	$\Delta\mathbf{q}_{n,i=0} = 0$ – increments of nodal displacements, which are equal to zero, when $i = 0$ on n-step of loading
12	$\Delta\mathbf{R}$ – vector of nodal forces resulting from the increment of external loading at this step
13	$\mathbf{Q}_{n-1}^{\text{unb}}$ – non-balanced part of external forces
14	$\mathbf{D}_{\text{pf},n}$ – plastic matrix of the plastic flow theory found by the dependence from [1, 16]
15	$A = 0$ – the parameter depending on strengthening, which is for ideal plastic material equals to zero
16	f – yield surface for an ideal elastic-plastic material
17	σ_s – yield strength
18	$\boldsymbol{\sigma}_{n-1}$ – full corrected elastic-plastic stresses at the previous n – 1 load step
19	**a** – column vector of derivatives of the yield surface f with respect to stresses

The stress $\boldsymbol{\sigma}$ for **a** and $f(\boldsymbol{\sigma})$ in (2) are total stresses. The relationships for $\mathbf{D}_{\text{pf},n}$ in (2) are true when $f(\boldsymbol{\sigma}) \geq 0$, and if $f(\boldsymbol{\sigma}) < 0$, then elastic deformation occurs, and all elements of the $\mathbf{D}_{\text{pf}}$ matrix are equal to zero. In this case, if $f(\boldsymbol{\sigma}) \geq 0$, then $\boldsymbol{\sigma}$ should be adjusted to ensure that the condition $f(\boldsymbol{\sigma}) = 0$ is satisfied. Model (1) provides the unloading to be taken into consideration automatically. The relationships for the FEM for total displacements and loads in the determination of both strains and nodal displacements are valid for their increments as well.

Within the theory of plastic flow, the complete external loading is divided into steps. The increments of the external loading are sequentially specified, and within each increment, an iterative process is performed for $\Delta\mathbf{q}_i$, $\Delta\mathbf{q}_{i-1}$.

Since there are no functional dependencies of the total quantities of stress-strain state (SSS) elements on the coordinates of the body points within the plasticity theory, calculations are performed in characteristic points, such as the nodes of FE and Gaussian integration points.

For carrying the part of calculations related to stress operations, an explicit modified Euler algorithm with substepping [1] had been implemented, where each load step is subdivided into substeps. There are auxiliary algorithms [1] associated with this algorithm are: Modified Regula-Falsi Intersection Scheme, Modified Regula-Falsi Intersection Scheme for Negative Plastic Multiplier, and the yield surface correction scheme. These algorithms are related to stress adjustment when they exceed the plasticity surface f. Since the elastic-plastic calculations are applied to metal-type materials, the plasticity surface and plastic potential involved in [1] are determined by the same dependencies as described in the mathematical model of plastic flow theory. The mentioned modified Euler algorithm belongs to second-order schemes.

In the course of the research, soft cyclic loading was implemented. The material of the beam-wall is ideal elastic-plastic, with a horizontal yield area, possessing the following mechanical characteristics: yield strength $\sigma_s = 235$ MPa, Young's modulus $E = 2 \times 10^{11}$ Pa, Poisson's ratio $\mu = 0.3$, which approximately corresponds to the characteristics of St3 steel.

Before processing the calculations, the convergence of the calculated components of the stress-strain state depending on the sizes of FE and the load step (for the plastic problem) was investigated. The necessary maximum sizes of FE and load step were determined, at which the

calculated values of the stress-strain state components stabilize. Further reduction in the sizes of FE and/or the load step does not cause significant changes in the values of the stress-strain state components.

Table 2 shows a comparison of the ranges of cyclic elastic-plastic strains intensity ε_i in the stress concentrator of the beam-wall with parameters H/h=1,6; α=45°; r/h=0,05. In Table 2, strains ε_i are calculated using quadratic and cubic FE [13, 14] for different thicknesses and loads, where the difference between ε_i, %, is calculated relative to cubic FE.

Table 2

Comparison of ranges of cyclic strains for different FE

№	s/h	p/σ_s	Range of cyclic strains ε_i		Difference, %
			Quadratic FE [13]	Cubic FE [14]	
1	0,02	0,48	6,784E-03	6,761E-03	-0,35
2		0,69	1,717E-02	1,676E-02	-2,44
3	0,04	0,48	6,326E-03	6,281E-03	-0,71
4		0,69	1,655E-02	1,592E-02	-3,95

As we can see from Table 2, the FE type practically does not affect the values of elastic-plastic strains.

To check the fact of volumetric closure, external loading was applied close to 0.9 of the yield limit σ_s (p/σ_s = 0.9). For each loading step, the number of iterations increased from 15–25 to 40–60, which may indirectly indicate the onset of volumetric closure. With external loads of p/σ_s = 0.9, the radius of the plastic zone, measured from the dangerous stress concentrator point, is approximately h/4, and the rest of the material remains in the elastic state. Thus, the majority of the material of the beam-wall remains in the elastic state under a loading of p/σ_s = 0.9, indicating the absence of volumetric closure effect. This applies to FE with 10 and 20 nodes.

5.2. Study of the influence of load vector balancing on static and cyclic ranges of elastic-plastic strains. Within the scope of this research, cyclic deformation diagrams in the critical point of the stress concentrator *6* of the steel beam-wall (Figure 1) were obtained through calculations using the plastic yield model (1). The concentrator undergoes elastic-plastic deformation conditions. Cyclic diagrams in this article were obtained and presented for the beam-wall with fixed parameters:

$$H/h = 1{,}6;\ \alpha=45°;\ r/h=0{,}1;\ p/\sigma_s=0{,}713879, \qquad (4)$$

to study the influence of the unbalanced part Q_{n-1}^{unb} in (1). Cyclic loading p=p1 corresponds to tension-compression. The computational scheme of the beam-wall is shown in Figure 2.

When using the computational scheme in Figure 2 for the beam-wall, the most critical SSS is implemented. The justification for the design model in Figure 2 is as follows. The presence of the attached sheating's flange I (Figure 1) determines the position of the neutral layer of the beam-wall closer to edge 2. The wider the attached sheating's flange, then the closer the neutral layer of the beam-wall situated to edge 2, and the greater stresses in the concentrator 6 (Figure 1, 2) take place. As the width of the attached sheating's flange approaches infinity, the neutral layer coincides with edge 2. For tension-compression p1, the stress values in the concentrator 6 (Figure 1, 2) are always greater than for bending p2, under equal conditions. In this case, the computational scheme provides the most unfavorable and dangerous SSS.

The cyclic loading scheme is shown in Figure 3, where: c – one loading cycle; t – pseudo time; I – loading path (solid line), when tension p occurs initially in the first cycle; II – loading path (dashed line), when compression p occurs initially in the first cycle.

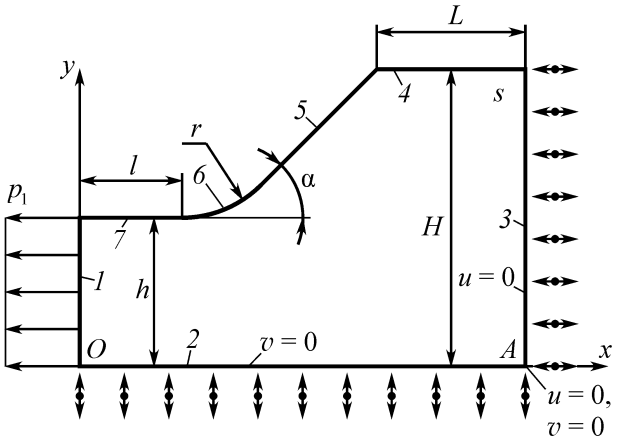

Figure 2. The design scheme of the beam-wall under tension-compression

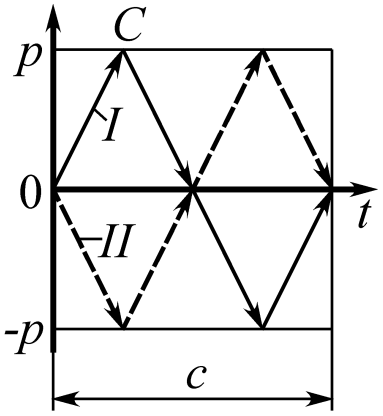

Figure 3. The beam-wall's loading way

In Figure 4, cyclic diagrams are shown, obtained without considering corrections Q_{n-1}^{unb} for parameters (4). The cyclic loading p applied to edge 1 (Figure 2) is symmetrical [–p; +p] (Figure 3).

These diagrams are plotted in coordinates εi – σi (where σi is in MPa), meaning «strain intensity» – «stress intensity» (according to Mises), where the signs of εi and σi were traced based on the signs of their component parts.

Point C in Figure 3 corresponds to point C in Figure 4 and corresponds to the condition of a single static loading from 0 to p (or to –p). As we can see from Figure 4, the type of initial loading of the 1st cycle (tension or compression) does not affect the width of the hysteresis loop for an ideal elastic-plastic material. The first cycle follows the path ABCDEF, and the subsequent cycles follow a closed path FGHE, forming the hysteresis loop of the cyclic deformation diagram.

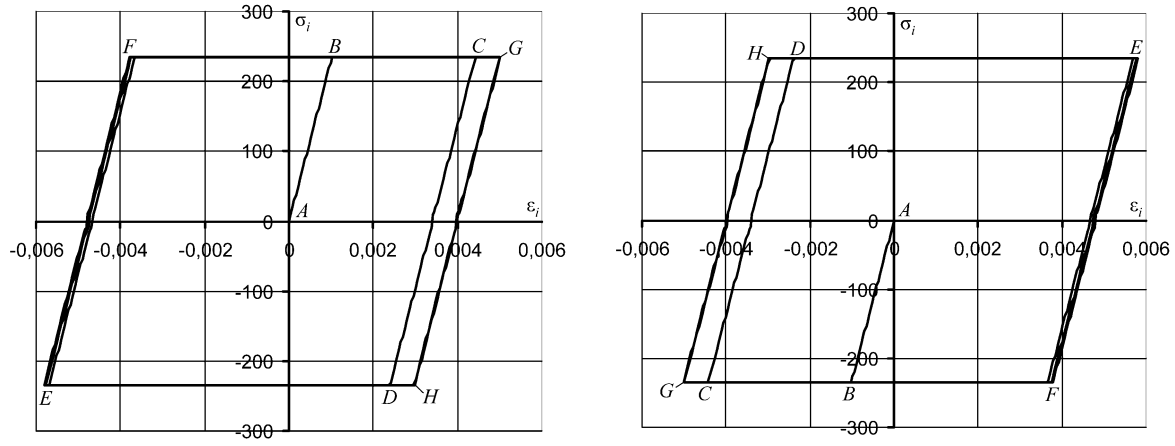

Figure 4. Cyclic diagrams for symmetric cycle of external loading without considering Q_{n-1}^{unb}: *a* – the loading type *I* (fig. 3); *b* – the loading type *II* (fig. 3)

The cyclic diagrams shown were obtained for 3 cycles. Along the line EF, a slight material softening can be observed after each cycle. After the 3rd cycle, there is practical stabilization of the hysteresis loop width. Material running-in occurs during the 1st cycle. The higher the load and stress concentration in the concentrator, the more cycles of loading are needed to stabilize the hysteresis loop of the cyclic diagram.

For the considered example (Figure 4), the value of elastic-plastic strains calculated by the FEM under single loading from 0 to p in point C is εiC=0,0046449. The values of elastic-plastic strains in the most distant points E and G of the cyclic diagram are: εiE = –0,0050132; εiG = 0,00581403 respectively. The cyclic range of the diagram is εi cycle=εiE – εiG=0,010827205. The static range is εi stat = 2 εiC = 0,009289787. The cyclic range is 16% greater than the static range. For the same beam-wall, but for a lower external loading p/σs=0,527763 the cyclic range exceeds the static one by 11%. Thus, an increase in external loading p leads to an increase in the difference between static and cyclic strains' ranges, with the cyclic range always being greater. For instance, for the beam-wall with different parameters: H/h = 2,4; α = 75°; r/h = 0,05; p/σs = 0,674, the cyclic range exceeds the static one by 14.4%. Based on the analysis of the elastic-plastic strains of selected beam-wall variants, it was concluded that for p/σs ≤ 0,65 the cyclic range of elastic-plastic strains does not exceed 15% of the static range.

Figure 5 shows the cyclic deformation diagram obtained with the application of correction Q_{n-1}^{unb} in the eqaution (1), for the parameters fig. 4, a.

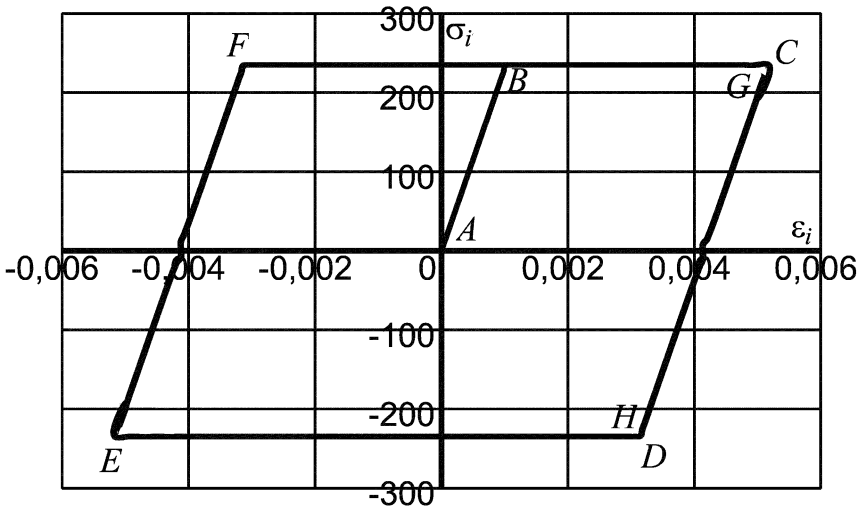

Figure 5. The cyclic diagram for the symmetrical cycle of external loading considering Q_{n-1}^{unb} in (1)

The cyclic diagram in Figure 5 is symmetric. Point C coincides with point G, and point D with point H. The static range of elastic-plastic strains in this case corresponds to the cyclic one and is εi cycle=εiE–εiG=0,010351, which is 4.4% less than the cyclic range εi cycle=0,010827205, obtained without applying Q_{n-1}^{unb} in the equation (1).

Thus, when applying the correction Q_{n-1}^{unb} in equation (1) the static range of elastic-plastic strains will be slightly overrated by 5–16% (for p/σs ≤ 0,9), while the cyclic range will be understated by 4–8% (for p/σs ≤ 0,65), compared to not applying Q_{n-1}^{unb}. Since the cyclic range of elastic-plastic strains is of primary interest, it can be said that not applying

the correction Q_{n-1}^{unb} will yield safer results, albeit slightly conservative. Applying Q_{n-1}^{unb} provides more accurate results but increases calculation time for single loading.

5.3. Study of the influence of thickness on the ranges of cyclic elastic-plastic deformations strains. The section under discussion investigates the effect of thickness s on the values of cyclic elastic-plastic deformations strains at in the critical stress concentrator point of the beam-wall under cyclic symmetric loading $p = p_1$, [17]. Under elastic deformation, the components of stresses at in the stress concentrator 6 (Figure 1) of the beam-wall practically do not depend on the thickness s. In this case, a two-dimensional stress state is realized for the beam-wall in Figure 1. However, under conditions of elastic-plastic deformation, the influence of thickness s on the values of elastic-plastic deformations strains at in the concentrator 6 (Figure 1) was observed. In the latter case, a purely two-dimensional stress state is no longer fully realized, and complex deformation processes associated with the formation and development of the plastic zone occur.

The research was conducted for a the steel beam-wall with fixed parameters: H/h=1,6; r/h=0,05; α = 45°. The relative thickness s/h varied from 0,02 to 0,32. These fixed geometric parameters ensure high values of the ranges of cyclic elastic-plastic deformations strains to qualitatively study the influence of thickness s.

Figures 6 and 7 present graphs illustrating the dependence of the intensity of cyclic elastic-plastic deformations strains εi in the concentrator 6 (fig. 1) on the relative thickness s/h and the relative external loading p/σs.

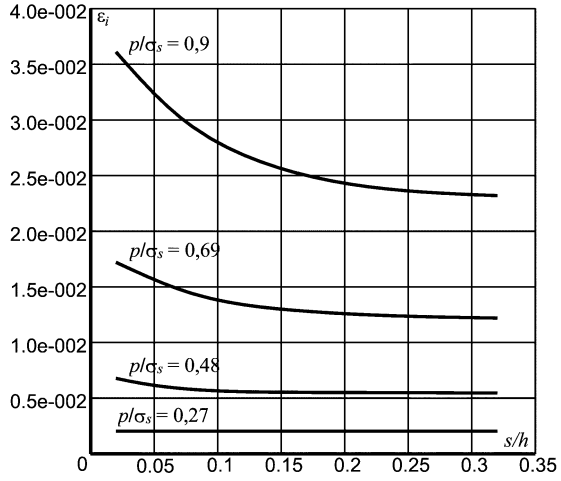

Figure 6. The influence of the relative thickness s/h onto the range of cyclic elastic-plastic strains εi in the stress concentrator for the different levels of cyclic relative loading p/σs

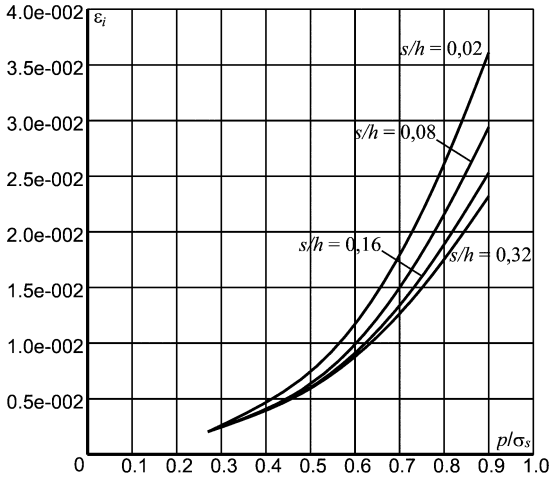

Figure 7. The influence of cyclic loading p/σs onto the range of cyclic elastic-plastic strains εi in the stress concentrator for different values of the relative thickness s/h

Analyzing the graphs in figures 6 and 7, the following can be said. It had been observed, that there is an increase of the influence of thickness s on the strains' range εi as the load p increases. Gradual reduction of thickness s (or s/h) leads to an increase of the ranges of cyclic strains εi for a fixed value of load p (or p/σs). For an external load p/σs = 0,9 gradual reduction of thickness s from s/h = 0,32 to s/h = 0,02 (a 16-fold decrease) results in an 50÷60% increasing of the range εi (approximately 1.5 to 1.6 times). For a thickness s/h = 0,02 increasing the load p/σs from 0,27 to 0,9 (almost threefold increase)

leads to an almost 17 to 20-fold increase in the range of elastic-plastic cyclic strains εi (fig. 7). However, for the thickness s/h = 0,32 (which is 16 times greater than the previous thickness s/h = 0,02) the same change in external load results in an increase of strains magnitudes εi only approximately 10 times. Gradual increase of thickness s/h softens (neutralizes or gradually reduces) the influence of load p/σs on the ranges εi. For each geometry variant of the beam-wall, there is an upper limit of thickness s/h exists, at which stabilization of εi occurs, and further increase of s/h does not lead to a change in εi. The upper limit of thickness s/h (or s), when it does not affect the values of strains εi depends on the parameters H/h, r/h, α and p/σs. Thus, all these parameters are interrelated. For very thick beam-walls, where there is no influence of s/h, ranges εi are the smallest among all possibilities. Applying a two-dimensional problem for the beam-wall in elastic-plastic calculations yields the highest values of strains εi among all possibilities. Furthermore, the two-dimensional problem does not consider all components of the stress tensor, and, as already mentioned in the literature review, the influence of the type of two-dimensional stress state (plane strain or plane stress state) on the ranges of strains is not fully understood.

In works [6, 7, 8], through experimental and theoretical studies, it had been shown that the shape of plastic zones and the magnitude of strains depend on the thickness of the plate. Stress concentrators like 6 (Figure 1) can be considered as zero-length cracks. During the initial growth of the plastic zone in the notch/crack, when the characteristic dimensions of the plastic zone are smaller than the plate thickness, the process of elastic-plastic deformation is volumetric. In this case, the plastic zone develops along the crack. However, when the dimensions of the plastic zone are comparable to the thickness of the wall, a change in the mechanism of plastic zone development occurs. A plane stress state occurs relative to the plastic zone. Thus, in [8], it was concluded that there is a transition from plane strain to plane stress state in the development of plastic zones. These are indirect evidence that the stabilization effect of thickness s on strains εi is associated with the aforementioned processes of plastic zone development. Let's explain how exactly it takes place. The smaller the thickness s, the faster/earlier the transition from plane strain to plane stress state occurs. For example, for a load p/σs = 0.27 (Figure 6), the thickness s/h does not affect the ranges of εi, because the dimensions of the plastic zone in this case are always smaller than the thickness s/h, and therefore there is no transition from a state of plane strain (volumetric SSS) to plane stress state.

Conclusions. Based on the results in Table 2, it can be concluded that the type of finite element (FE) practically does not affect the parameters of elastic-plastic deformation in point. This is supported by findings in [16], where it is noted that the results of elastic-plastic deformation calculation depend more on the quality of information processing in characteristic points (integral and nodal points) than on the type of FE. When using FE with 10 and 20 nodes for loads close to p/σs = 0.9, volumetric closure was not observed. For operational cases, the beam-wall operates under loads smaller than p/σs = 0.9, ensuring the absence of volumetric closure effect in practical calculations.

Balancing the right-hand side using Q_{n-1}^{unb} in (1) improves the results of the characteristics of elastic-plastic deformation under static single loading, but slightly increases the computation time. During cyclic loading, consideration of Q_{n-1}^{unb} does not significantly refine the results but stabilizes the cyclic diagram practically after the 1st cycle, whereas the absence of balancing Q_{n-1}^{unb} stabilizes after a larger number of cycles (3 cycles for the investigated case). Further additional research is needed to obtain quantitative characteristics of computation time savings.

It had been found that the wall thickness s affects the parameters of elastic-plastic strains in the stress concentrator 6 (Figure 1). Decreasing the thickness s/h increases the magnitude of elastic-plastic (both static and cyclic) strains εi for the same fixed level of external loading and geometry. The influence of thickness s on elastic-plastic strains εi increases with increasing external loading p. Increasing s/h mitigates the effect of loading p/σs on the range of εi.

References

1. Andrew John Abbo B.E. Finite Element Algorithms For Elastoplasticity And Consolidation: 3-rd ed. *A Thesis submitted for the Degree of Doctor of Philosophy at the University of Newcastle*. 2005. 285 p.
2. Sumelka W., & Nowak M. On a general numerical scheme for the fractional plastic flow rule. *Mechanics of Materials*. Netherlands: Elsevier, 2018, vol. 116, pp. 120–129. https://doi.org/10.1016/j.mechmat.2017.02.005
3. Lu D., Liang J., Du X., Ma C., & Gao Z. Fractional elastoplastic constitutive model for soils based on a novel 3D fractional plastic flow rule. *Computers and Geotechnics*. UK: Elsevier BV, 2019, vol. 105, pp. 277–290. https://doi.org/10.1016/j.compgeo.2018.10.004
4. Wang J., Liu K., & Zhang D. An improved CE/SE scheme for multi-material elastic–plastic flows and its applications. *Computers & Fluids*. UK: Elsevier Ltd., 2009, vol. 38 (3), pp. 544–551. https://doi.org/10.1016/j.compfluid.2008.04.014
5. Wells G. N., Sluys L. J., & de Borst R. A p-adaptive scheme for overcoming volumetric locking during plastic flow. *Computer Methods in Applied Mechanics and Engineering*. Netherlands: Elsevier, 2002, vol. 191 (29–30), pp. 3153–3164. https://doi.org/10.1016/S0045-7825(02)00252-9
6. Swedlow, Jerold Lindsay. The thickness effect and plastic flow in cracked plates. *Dissertation (Ph.D.)*. 1965. California Institute of Technology. Doi: 10.7907/0WVE-W364.
7. Beynet P., & Plunkett R. Plate impact and plastic deformation by projectiles. *Experimental Mechanics*. US: Springer New York, 1971, no. 11, pp. 64–70. https://doi.org/10.1007/BF02320622
8. Parton V. 3., Morozov E. M. Mehanika uprugoplasticheskogo razrusheniya. 2-e izd., pererab. i dop. M.: Nauka, Glavnaya redakciya fiziko-matematicheskoj literatury, 1985. 504 p. [In Russian].
9. Zhang Y.-Q., Hao H., & Yu M.-H. A Unified Characteristic Theory for Plastic Plane Stress and Strain Problems. Journal of Applied Mechanics. US: ASME, 2003, vol. 70 (5), pp. 649–654. https://doi.org/10.1115/1.1602484
10. Runesson K., Saabye Ottosen N., & Dunja P. Discontinuous bifurcations of elastic-plastic solutions at plane stress and plane strain. International Journal of Plasticity. UK: Elsevier Ltd., 1991, vol. 7 (1–2), pp. 99–121. Doi: 10.1016/0749-6419(91)90007-l
11. Sergei Alexandrov, Yeau-Ren Jeng. A method of finding stress solutions for a general plastic material under plane strain and plane stress conditions. *Journal of Mechanics*. UK: Cambridge University Press, 2021, vol. 37, pp. 100–107. https://doi.org/10.1093/jom/ufaa001
12. Eraslan A. N., Akis T. On the plane strain and plane stress solutions of functionally graded rotating solid shaft and solid disk problems. *Acta Mechanica*. Austria: Springer-Verlag Wien, 2006, vol. 181, pp. 43–63. https://doi.org/10.1007/s00707-005-0276-5
13. Sokov V. M. "Bibliotechnij klas FE VolumeProblemOfTheoryOfElasticity Tetrahedron 10Nodes": a.s. № 109597 Ukrayini vid 18.11.2021. Avtorske pravo i sumizhni prava. Byuleten no. 68, 2021, pp. 262–263. [In Ukrainian].
14. Sokov V. M. "Bibliotechnij klas FE_VolumeProblemOfTheoryOfElasticity_Tetrahedron_20Nodes": a. s. № 116226 Ukrayini vid 30.01.2023. Avtorske pravo i sumizhni prava. Byuleten no. 74, 2023, pp. 309–310. [In Ukrainian].
15. Postnov V. A., Harhurim I. Ya. Metod konechnyh elementov v raschetah sudovyh konstrukcij. L.: Sudostroenie, 1974. 344 p. [in Russian]
16. Zienkiewicz O. C., Taylor R. L. The Finite Element Method for Solid and Structural Mechanics: 6-th ed. Elsevier, 2005. 648 p.
17. Sokov V. M. Study of influence of the thickness in the stress raiser of the ship structure assembly in plastic stage. Suchasni tekhnolohii proektuvannia, pobudovy, ekspluatatsii i remontu suden, morskykh tekhnichnykh zasobiv i inzhenernykh sporud: proceedings of all-Ukrainian scientific and technical conference with international participation (Mykolaiv, 17–18 may 2023 y.). Mykolaiv: NUOS, 2023. pp. 103–107.

Список використаних джерел

1. Andrew John Abbo B. E. Finite Element Algorithms For Elastoplasticity And Consolidation: 3-rd ed. *A Thesis submitted for the Degree of Doctor of Philosophy at the University of Newcastle*. 2005. 285 p.

2. Sumelka, W., & Nowak, M. On a general numerical scheme for the fractional plastic flow rule. *Mechanics of Materials*. Netherlands: Elsevier. 2018. Vol. 116. P. 120–129. https://doi.org/10.1016/j.mechmat.2017.02.005
3. Lu D., Liang J., Du X., Ma C., & Gao Z. Fractional elastoplastic constitutive model for soils based on a novel 3D fractional plastic flow rule. *Computers and Geotechnics*. UK: Elsevier BV. 2019. Vol. 105. P. 277–290. https://doi.org/10.1016/j.compgeo.2018.10.004
4. Wang J., Liu K., & Zhang D. An improved CE/SE scheme for multi-material elastic–plastic flows and its applications. *Computers & Fluids*. UK: Elsevier Ltd., 2009. Vol. 3 (3). P. 544–551. https://doi.org/10.1016/j.compfluid.2008.04.014
5. Wells G. N., Sluys L. J., & de Borst R. A p-adaptive scheme for overcoming volumetric locking during plastic flow. *Computer Methods in Applied Mechanics and Engineering*. Netherlands: Elsevier, 2002. Vol. 191 (29–30). P. 3153–3164. https://doi.org/10.1016/S0045-7825(02)00252-9
6. Swedlow, Jerold Lindsay. The thickness effect and plastic flow in cracked plates. *Dissertation (Ph.D.)*. 1965. California Institute of Technology. Doi: 10.7907/0WVE-W364.
7. Beynet P., & Plunkett R. Plate impact and plastic deformation by projectiles. *Experimental Mechanics*. US: Springer New York. 1971. No. 11. P. 64–70. https://doi.org/10.1007/BF02320622
8. Партон В. З., Морозов Е. М. Механика упругопластического разрушения. 2-е изд., перераб. и доп. М.: Наука, Главная редакция физико-математической литературы, 1985. 504 с.
9. Zhang Y.-Q., Hao H., & Yu M.-H. A Unified Characteristic Theory for Plastic Plane Stress and Strain Problems. *Journal of Applied Mechanics*. US: ASME, 2003. Vol. 70 (5). P. 649–654. https://doi.org/10.1115/1.1602484
10. Runesson K., Saabye Ottosen N., & Dunja P. Discontinuous bifurcations of elastic-plastic solutions at plane stress and plane strain. International Journal of Plasticity. UK: Elsevier Ltd., 1991. Vol. 7 (1–2). P. 99–121. https://doi.org/10.1016/0749-6419(91)90007-L
11. Sergei Alexandrov, Yeau-Ren Jeng. A method of finding stress solutions for a general plastic material under plane strain and plane stress conditions. *Journal of Mechanics*. UK: Cambridge University Press, 2021. Vol. 37. P. 100–107. https://doi.org/10.1093/jom/ufaa001
12. Eraslan A. N., Akis T. On the plane strain and plane stress solutions of functionally graded rotating solid shaft and solid disk problems. *Acta Mechanica*. Austria: Springer-Verlag Wien, 2006. Vol. 181. P. 43–63. https://doi.org/10.1007/s00707-005-0276-5
13. Соков В. М. «Бібліотечний клас FE VolumeProblemOfTheoryOfElasticity Tetrahedron 10Nodes»: а.с. № 109597 України від 18.11.2021. / Авторське право і суміжні права. Бюлетень № 68, 2021. С. 262–263.
14. Соков В. М. «Бібліотечний клас FE_VolumeProblemOfTheoryOfElasticity_Tetrahedron_20Nodes»: а. с. № 116226 України від 30.01.2023. Авторське право і суміжні права. Бюлетень № 74, 2023. С. 309–310.
15. Постнов В. А., Хархурим И. Я. Метод конечных элементов в расчетах судовых конструкций. Л.: Судостроение, 1974. 344 с.
16. Zienkiewicz O. C., Taylor R. L. The Finite Element Method for Solid and Structural Mechanics: 6-th ed. Elsevier, 2005. 648 p.
17. Sokov V. M. Study of influence of the thickness in the stress raiser of the ship structure assembly in plastic stage. Suchasni tekhnolohii proektuvannia, pobudovy, ekspluatatsii i remontu suden, morskykh tekhnichnykh zasobiv i inzhenernykh sporud: proceedings of all-Ukrainian scientific and technical conference with international participation (Mykolaiv, 17–18 may 2023 y.). Mykolaiv: NUOS, 2023. pp. 103–107.

УДК 539.4 : 629.5

ВИВЧЕННЯ ВПЛИВУ СУПУТНІХ ФАКТОРІВ НА ХАРАКТЕРИСТИКИ ПРУЖНО-ПЛАСТИЧНОГО ДЕФОРМУВАННЯ КОНЦЕНТРАТОРА НАПРУЖЕНЬ БАЛКИ-СТІНКИ ЗІ ЗЛАМОМ КРОМОК

Валерій Соков

Національний університет кораблебудування імені адмірала Макарова, Миколаїв, Україна

Резюме. *Досліджено тонкостінну сталеву балку-стінку зі зламом кромок, яка входить до складу багатьох конструкцій. Стінка цієї балки складається з двох призматичних частин з прямолінійним переходом від меншої висоти стінки до більшої, утворюючи разом з кромками призматичних частин ламану верхню кромку. Нижня прямолінійна кромка стінки кріпиться до обшивки. На балку-стінку діють статичні та циклічні навантаження, при яких у концентраторі напружень можуть виникати пружно-пластичні деформації. Це спричиняє невиконання статичної міцності та ріст втомних тріщин. Фактори, які впливають на параметри пружно-пластичного деформування в концентраторі цієї балки, практично не вивчені. Представлено результати дослідження впливу товщини балки-стінки та балансування вектора навантажень на значення статичних та циклічних розмахів пружно-пластичних деформацій у концентраторі напружень. Виявлено, що балансування вектора навантажень значно покращує результати пружно-пластичних деформацій при однократному статичному навантаженні й дозволяє застосовувати більший крок навантаження для отримання тих же результатів, ніж за відсутності балансування. Застосування балансування вектора навантажень призводить до стабілізації петлі циклічних деформацій практично з 1-го циклу. Якщо балансування відсутнє, то стабілізація відбувається тільки з 3-го циклу. На відміну від статичних, значення циклічних розмахів не залежить від застосування чи незастосування балансування, і залишається практично стабільним при фіксованих геометричних параметрах та навантаженні. Поступове зменшення товщини балки-стінки викликає ріст розмаху (статичних і циклічних) пружно-пластичних деформацій у концентраторі напружень. Отримані результати скоротять час при плануванні серійних розрахунків пружно-пластичного деформування балки-стінки зі зламом кромок з метою створення відповідних методик проєктування.*

Ключові слова: *пружно-пластичне деформування, циклічні діаграми, балка зі зламом кромок, скінченні елементи.*

https://doi.org/10.33108/visnyk_tntu2024.02.060 *Отримано 27.03.2024*